Extramedullary multiple myeloma with central nervous system and multiorgan involvement: Case report and literature review

Weiyong Lee[1,2*], Robert Chun Chen[2,4], Saravana Kumar Swaminathan[3,4], Chi Long Ho[1,4,5]

1. Department of Radiology, Sengkang General Hospital, Singapore

2. Department of Diagnostic Radiology, Singapore General Hospital, Singapore

3. National Neuroscience Institute, Singapore

4. Duke-NUS Graduate Medicine School, Singapore

5. Lee Kong Chian School of Medicine, Singapore

* **Correspondence:** Weiyong Lee, MBBS, Department of Diagnostic Radiology, Singapore General Hospital, Singapore (*weiyong.lee@mohh.com.sg*)

Radiology Case. 2019 Dec; 13(12):1-12 :: DOI: 10.3941/jrcr.v13i12.3784

ABSTRACT

Multiple myeloma is a hematologic malignancy due to monoclonal plasma cell proliferation. It is usually confined to the bone marrow, although extramedullary involvement is known to occur in almost any organ system; myelomatous spread to the central nervous system is a rare manifestation of myeloma. Extramedullary disease is thought to be related to hematogenous spread when myeloma cells show decreased cell surface receptor expression, allowing cells to escape from the bone marrow. Disease outside of the bone marrow generally indicates a poor prognosis; central nervous system involvement is associated with a median prognosis of less than 6 months, thereby requiring more aggressive treatment paradigms. We herein describe an unusual case of a patient with extramedullary multiple myeloma with central nervous system and multiorgan involvement. Despite an aggressive treatment strategy, the patient died a few months later after the initial diagnosis. The etiology, diagnostic criteria, clinical presentation, radiological features and differential diagnosis of this patient with extramedullary multiple myeloma are discussed here. The current treatment strategies are also briefly discussed.

CASE REPORT

CASE REPORT

A 64-year-old ethnic Malay man presented to a General Practitioner with a progressively enlarging and painful sternal lump yet was otherwise asymptomatic. The patient had no significant background medical or family history. The physical examination confirmed the presence of the sternal lump but was otherwise unremarkable. He was discharged from the outpatient clinic and referred for specialist review at a tertiary center. Two weeks later, he presented to the emergency department with altered mental status. The laboratory results showed elevated serum calcium of 2.78 mmol/L (reference range, 2.09-2.46 mmol/L). The full blood count, other serum electrolytes (including creatinine), and liver function tests were normal. Serum electrophoresis showed marked monoclonal IgA elevation. It showed elevated

gamma globulin of 43 g/L (reference range, 7-16 g/L) with a monoclonal band, reduced albumin of 31 g/L (reference range, 40-51 g/L), normal alpha-1 globulin, normal alpha-2 globulin and normal beta-globulin. There was elevated serum IgA 43.07(reference range, 0.47-3.59 g/L), normal serum IgG, normal serum IgM, elevated serum lambda free light chain of 321 mg/L (reference range, 5.7-26.3 mg/L) and normal serum Kappa free light chain. Immunofixation showed monoclonal gammopathy IgA λ type.

A contrast-enhanced computed tomography (CT) of the brain (Figure 1) was performed to investigate the cause of his altered mental state and it demonstrated multiple avidly enhancing dural based lesions adjacent to the supratentorial brain; the largest of the lesions showed indentation of the adjacent temporal lobe with marked perilesional edema and mass effect. In addition, there were diffuse osteolytic lesions throughout the calvarium.

Subsequent investigations were performed over the course of two weeks while the patient was in hospital.

The radiographic skeletal survey (Figure 2) demonstrated multiple "punched-out" lytic osseous lesions in the skull, radius, and ulna.

Contrast-enhanced magnetic resonance imaging (MRI) of the brain (Figure 3), corroborated the dural based lesions; there were linear and more nodular areas of pachymeningeal enhancement. No leptomeningeal or intraaxial disease was seen. In addition, there were centrally enhancing soft tissue masses in the paranasal sinuses and nasopharynx. Similar to the CT, multiple osseous lesions were noted throughout the calvarium.

A contrast-enhanced CT scan of the chest, abdomen, and pelvis (Figure 4) was performed. The chest revealed a 4.9 cm soft tissue mass centered in the sternum, several pulmonary nodules, and left axillary lymphadenopathy. The abdomen showed masses adjacent to both kidneys and bilateral adrenal masses.

A whole-body 18F-Fluorodeoxyglucose positron emission tomography/computed tomography (FDG PET/CT) scan (Figure 5) revealed the aforementioned masses to be hypermetabolic.

Histopathological examination of the soft tissue mass at the sternum obtained through an excisional biopsy revealed the presence of plasma cells consistent with multiple myeloma. (Figure 6). Histology of bone marrow biopsy revealed sheets of immature plasma cells occupying approximately 30-40% of the marrow cell population and approximately 20-30% of the inter-trabecular space confirming myeloma (Figure 6).

TREATMENT

The treatment began after all the above investigations were performed and the diagnosis confirmed. The patient was first treated with whole-brain radiation therapy of 20 Gy in 5 fractions, followed by an intrathecal chemotherapy regimen which was started for cytoreduction consisting of bortezomib in combination with dexamethasone, cyclophosphamide, etoposide, and cisplatin.

OUTCOME AND FOLLOW-UP

A follow up contrast-enhanced MRI brain, taken one month after the start of radiochemotherapy, showed decrease in size of the dural lesions with the corresponding reduction in the adjacent perilesional edema and mass effect (Figure 7). However, during a subsequent infusional chemotherapy session, he developed neutropenic sepsis with pneumonia secondary to cytomegalovirus infection. He was admitted to the intensive care unit and put on the ventilator but died a few days later from worsening sepsis and acute respiratory distress syndrome. He survived only 75 days after the initial diagnosis of the disease.

DISCUSSION

ETIOLOGY & DEMOGRAPHICS:

Multiple myeloma (MM) is a hematologic malignancy as a result of monoclonal proliferation of bone marrow plasma cells (Table 1). Globally, it has an age-standardized incidence rate of 2.1 per 100 000 persons with an age-standardized death rate of 1.5 per 100 000 persons [1]. MM has a slight male predilection and a median age of presentation of MM 66 years [2]; its incidence proportionally increases with age. The risk factors for MM include advanced age, African American ethnicity, positive family history, obesity and history of monoclonal gammopathy of undetermined significance (MGUS) or solitary plasmacytoma [3]. It has been shown that virtually all cases of MM are preceded by MGUS, an asymptomatic non-malignant condition confined to the bone marrow and skeleton [4]. Extramedullary multiple myeloma (EM) [5] can involve any systemic organ and is seen in 10-16% of myeloma cases [6]. It has a higher male to female ratio than typical MM (1.9 vs 1.1, respectively) [4]. Central nervous system (CNS) involvement is very rare and is only seen in 0.7% of myeloma cases; CNS involvement portends a poor prognosis [7].

According to Bladé et al, EM may have two different origins: 1) direct mechanical extension from the bone marrow when they disrupt the cortical bone and spread into the adjacent soft tissues or 2) hematogenous metastatic spread when the decrease of selected cell surface adhesion receptors allows for bone marrow release [8]. Paludo et al. suggested that extramedullary spread in MM could be due to a sub-selection of plasma cell clones able to survive outside of the medullary cavity following successful initial treatment with novel agents, monoclonal antibodies and autologous stem cell transplant [7]. EM rates are reported higher now than in the past, likely related to the widespread use CT, MRI and FDG PET/CT, which are now accepted as diagnostic alternatives to plain radiographs for MM diagnosis [2, 4].

Histologically, EM usually consists of immature or plasmablastic cells as opposed to mature or plasmacytic cells in bone-related multiple myeloma. Patients with EM have

comparatively higher serum LDH levels, anemia and thrombocytopenia [9]. EM also tends to be non-secretory (absence of monoclonal protein in blood or urine) and demonstrate high-risk cytogenetic features. The molecular pathogenesis of EM is only partially understood. P53 tumour suppressor gene mutations, Ras oncogene mutations, upregulation of a focal adhesion kinase which has a tumor-promoting role in MM have been implicated [9]. There are also decreased expression of the CD56 adhesion molecule and increased expression of CD44, which are both involved in cell proliferation and migration. In addition to the cytological and molecular characteristics described above for EM, it appears that EM with CNS involvement tends to be of the IgA monoclonal subtype with deletions of 13q and 17p [3].

CLINICAL & IMAGING FINDINGS:

The most updated (2016) diagnostic criteria by the International Myeloma Working Group has established diagnostic criteria for MM and its related plasma cell disorders (e.g. Non-IgM monoclonal gammopathy of undetermined significance (MGUS), IgM MGUS, solitary plasmacytoma, etc.) [10]. The diagnosis of MM utilizes a combination of clinical, pathological, and radiological measures, with myeloma defining events succinctly captured by the CRAB acronym: elevated serum calcium, renal function impairment, anemia and/or bone involvement [10]. Of note, a bone marrow biopsy to demonstrate clonal marrow plasma cells or biopsy-proven bony or extramedullary plasmacytoma must be present.

The latest criteria for the radiological assessment of MM bone disease recommends the use of more advanced imaging techniques such as whole-body CT, MRI, and whole-body FDG PET/CT over that of radiographic bone survey. As many as 80% more lesions are seen on the newer imaging techniques [10].

The imaging appearance of EM is nonspecific and commonly presents with homogeneous soft tissues masses on CT which demonstrate hypermetabolism on FDG PET/CT. It most commonly affects the reticuloendothelial system such as the lymph nodes, spleen and liver. Other commonly affected areas include the abdominal organs such as the kidneys and small bowel, and head and neck regions [5]. Less commonly, it affects the chest as parenchymal nodules or masses, interstitial infiltration and pleural deposits [6].

Clinically, patients with CNS multiple myeloma may present with symptoms such as visual changes, radiculopathy, headache, confusion, dizziness, and seizures [3]. Compared to typical MM, CNS multiple myeloma has an earlier age of onset (53 vs 65-70 years old) [3]. Most of such cases tend to occur in patients during relapse or disease progression rather than the time of initial diagnosis [3]. The most common intracranial manifestations of CNS multiple myeloma on CT and MRI are pachymeningeal and leptomeningeal enhancing deposits followed by intraparenchymal brain lesions and direct extra-axial extension of disease from the adjacent bony calvarium [1, 7]. Some CNS multiple myeloma lesions may show susceptibility artifacts due to intralesional calcification, while others may mimic subdural hemorrhages [11]. A spinal tap, and cerebrospinal fluid cytology and flow cytometry may reveal plasma and monoclonal cell expansion in 87-91% of cases [3, 7].

TREATMENT & PROGNOSIS:

The treatment of MM continues to evolve at a rapid pace and has significantly improved patient survival [12]. However, EM often has a poor prognosis due to frequent treatment failure. Aggressive treatment strategies with a combination of conventional chemotherapy, proteasome inhibitors, immunomodulatory imide drugs, autologous stem cell transplant, and radiotherapy are often used [13, 14]. In the case of EM with CNS involvement, some authors advocate the use of craniocaudal irradiation and intrathecal and systemic combinational chemotherapy (e.g. methotrexate, cytosine arabinoside, idarubicin, and thiotepa); this combination crosses the blood-brain barrier hence allowing CNS penetration of chemotherapeutic agents [13].

EM is associated with a poor prognosis both at the time of diagnosis and during relapse, with an overall survival rate of 6 months during relapse [9]. In a study by Paludo et al, the median survival of myeloma patients with CNS involvement was 3.4 months [7].

DIFFERENTIAL DIAGNOSES:

Metastatic disease and central nervous system lymphoma are the most likely differential considerations for pachymeningeal nodular thickening. A less likely consideration would be hemangiopericytoma (Table 2). Inflammatory conditions such as neurosarcoidosis may also present with nodular pachymeningeal thickening, but a basilar leptomeningitis is the more classical finding.

Dural metastases

Advanced prostate, breast and lung malignancies are known to spread to the dura and other systemic organs [15]. Gastrointestinal, hematological, and head and neck malignancies less commonly spread to the pachymeninges. Imaging characteristics are similar to myeloma with CNS spread, and include diffuse and/or nodular pachymeningeal thickening, adjacent brain vasogenic edema, potential parenchymal invasion, and skull metastases. Often, metastatic disease to the dura will also have adjacent leptomeningeal spread of disease along the sulci.

Primary dural lymphoma

Primary dural lymphoma is a rare and distinctive subtype of primary CNS lymphoma which is reported to account for only 2.4% of primary CNS lymphoma [16]. Typically, primary dural lymphomas are of the mucosal associated lymphoid tissue (MALT) subtype, with high-grade diffuse large B-cell lymphoma accounting for the remainder. Key features to differentiate dural lymphoma from other processes include hyper-attenuation on CT, dark signal on T2, and restricted diffusion on DWI imaging (the aforementioned characteristics are related to dense cell packing) [17].

Primary intracranial tumors with extracranial dissemination

Solitary fibrous tumors, also known as hemangiopericytomas, are unusual extraaxial masses that are known to recur locally after surgical excision and spread outside of the intracranial cavity into multiple systemic organs. They tend to be multilobulated solitary lesions measuring >4 cm with homogeneous or heterogeneous enhancement. Adjacent perilesional edema and mass effect can be seen [18]. The extracranial spread of primary CNS solitary fibrous tumor may be related to breaching of the blood brain barrier following repeated surgeries for local excision or sarcomatous metaplasia after local radiation.

Neurosarcoidosis

Sarcoidosis is a systemic disease characterized by the formation of non-caseating granulomas. It is known to involve all part of the body; when it involves the brain and its coverings, it is termed neurosarcoidosis. Its imaging features are varied. It most commonly presents as leptomeningeal thickening and enhancement, seen in roughly 40% of cases. It is also known to affect the pachymeninges and present as focal dural masses or diffuse dural thickening [19]. The dural lesions typically enhance homogeneously on contrast-enhanced T1-weighted images and are dark on T2-weighted images. Other manifestations of neurosarcoidosis include intraparenchymal lesions, hypothalamus and pituitary involvement, cranial nerve extension, vasculitis and hydrocephalus.

Hypertrophic pachymeningitis

Hypertrophic pachymeningitis is a rare inflammatory disease that causes nodular thickening of the dura mater [17]. It can be idiopathic or secondary to infective/inflammatory causes., inclusive of rheumatoid arthritis, syphilis, granulomatosis with polyangiitis, tuberculosis, IgG4-related disease and carcinoma. On CT, it appears hyperdense. On MRI, the thickened dura is hypointense on T1-weighted and T2-weighted images with marked enhancement after contrast administration.

TEACHING POINT

Multiple myeloma is a plasma cell disorder primarily involving bone marrow. Occasionally, there is extramedullary involvement and in rare cases it involves the central nervous system. The imaging appearance of extramedullary multiple myeloma is typically that of homogeneous soft tissues masses on cross-sectional imaging, involving the reticuloendothelial system, abdominal organs (kidneys and small bowel), and head and neck region. Central nervous system multiple myeloma may manifest as pachymeningeal and leptomeningeal enhancing deposits, intraparenchymal brain lesions, and direct extra-axial extension from the adjacent calvarium.

REFERENCES

1. Cowan A, Allen C, Barac A et al. Global Burden of Multiple Myeloma A Systematic Analysis for the Global Burden of Disease Study 2016. JAMA Oncol. 2018;4(9):1221-1227. PMID: 29800065

2. Ferraro R, Agarwal A, Martin-Macintosh EL, Pellar PJ, Subramaniam RM. MR Imaging and PET/CT in Diagnosis and Management of Multiple Myeloma. RadioGraphics. 2015;35:438-454. PMID: 25763728

3. Jurczyszyn A, Grzasko N, Gozzetti A et al. Central Nervous System Involvement by Multiple Myeloma: a Multi-Institutional Retrospective Study of 172 Patients in daily clinical practice. Am J Hematol. 2016;91(6):575-80. PMID: 26955792

4. Varettoni M, Corso A, Pica G, Mangiacavalli S, Pascutto C, Lazzarino M. Incidence, presenting features and outcome of extramedullary disease in multiple myeloma: a longitudinal study on 1003 consecutive patients. Ann Oncol. 2010;21:325-330. PMID: 19633044

5. Ames J, Al-Samaraee A, Takaha T. Extraosseous Multiple Myeloma: Case Report of Presentation in the Lower Extremity Soft Tissues with Literature Review. ," Case Reports in Radiology. 2017;Article ID 9159035. PMID: 29391963

6. Hall M, Jagannathan JP, Ramaiya NH, Shinagare AB, Van den Abbeele AD. Imaging of Extraosseous Myeloma: CT, PET/CT, and MRI Features. American Journal of Roentgenology. 2010;195:1057-1065. PMID: 20966307

7. Paludo J, Painuly U, Kumar S et al. Myelomatous Involvement of the Central Nervous System. Clin Lymphoma Myeloma Leuk. 2016;16(11):644-654. PMID: 27624224

8. Bladé J, Fernández de Larrea C, Rosiñol L, Cibeira MT, Jimenez R, Powles R. Soft-Tissue plasmacytomas in multiple myeloma: incidence, mechanisms of extramedullary spread, and treatment approach. J Clin Oncol. 2011;29(28):3805-12. PMID: 21900099

9. Touzeau C, Moreau P. How I treat extramedullary myeloma. Blood. 2016;127(8):971-976. PMID: 26679866

10. Rajkumar SV. Updated diagnostic criteria and staging system for multiple myeloma. Am Soc Clin Oncol Educ Book. 2016;35:e418-e423. PMID: 27249749

11. Wirk B, Wingard J, Moreb J. Extramedullary disease in plasma cell myeloma: the iceberg phenomenon. Bone Marrow Transplantation. 2013;8(48):10-18. PMID: 22410751

12. Hanrahan CJ, Christensen CR, Crim J. Current Concepts in the Evaluation of Multiple Myeloma with MR Imaging and FDG PET/CT. RadioGraphics. 2010;30:127-142. PMID: 20083590

13. Valla K, Kaufman JL, Gleason C et al. Bortezomib in Combination with Dexamethasone, Cyclophosphamide, Etoposide, and Cisplatin (V-DCEP) for the Treatment of

Multiple Myeloma. Blood. 2014;124:2139. Retrieved from http://www.bloodjournal.org/content/124/21/2139

14. Varga G, Mikala G, Gopcsa L et al. Multiple Myeloma of the Central Nervous System: 13 Cases and Review of the Literature. J Oncol. 2018;23:3970169. PMID: 29849629

15. Nayak L, Abrey LE, Iwamoto FM. Intracranial Dural Metastases. Cancer. 2009 May 1;115(9): 1947-53. PMID: 19241421

16. Iwamoto FM, Abrey LE. Primary dural lymphomas: a review. Neurosurg Focus. 2006 Nov 15;21(5):E5. PMID: 17134121

17. Lim M, Kheok SW, Lim KC, Venkatanarasimha N, Small JE, Chen RC. Subdural haematoma mimics. Clinical Radiology. September 2019;74(9):663-675. PMID: 31109715

18. Chiechi MV, Smirniotopoulos JG, Mena H. Intracranial Hemangiopericytomas: MR and CT Features. Am J Neuroradiol. August 1996;17(7):1365-1371. PMID: 8871726

19. Smith JK, Matheus MG, Castillo M. Imaging Manifestations of Neurosarcoidosis. AJR Am J Roentgenol. 2004 Feb;182(2):289-95. PMID: 14736648

FIGURES

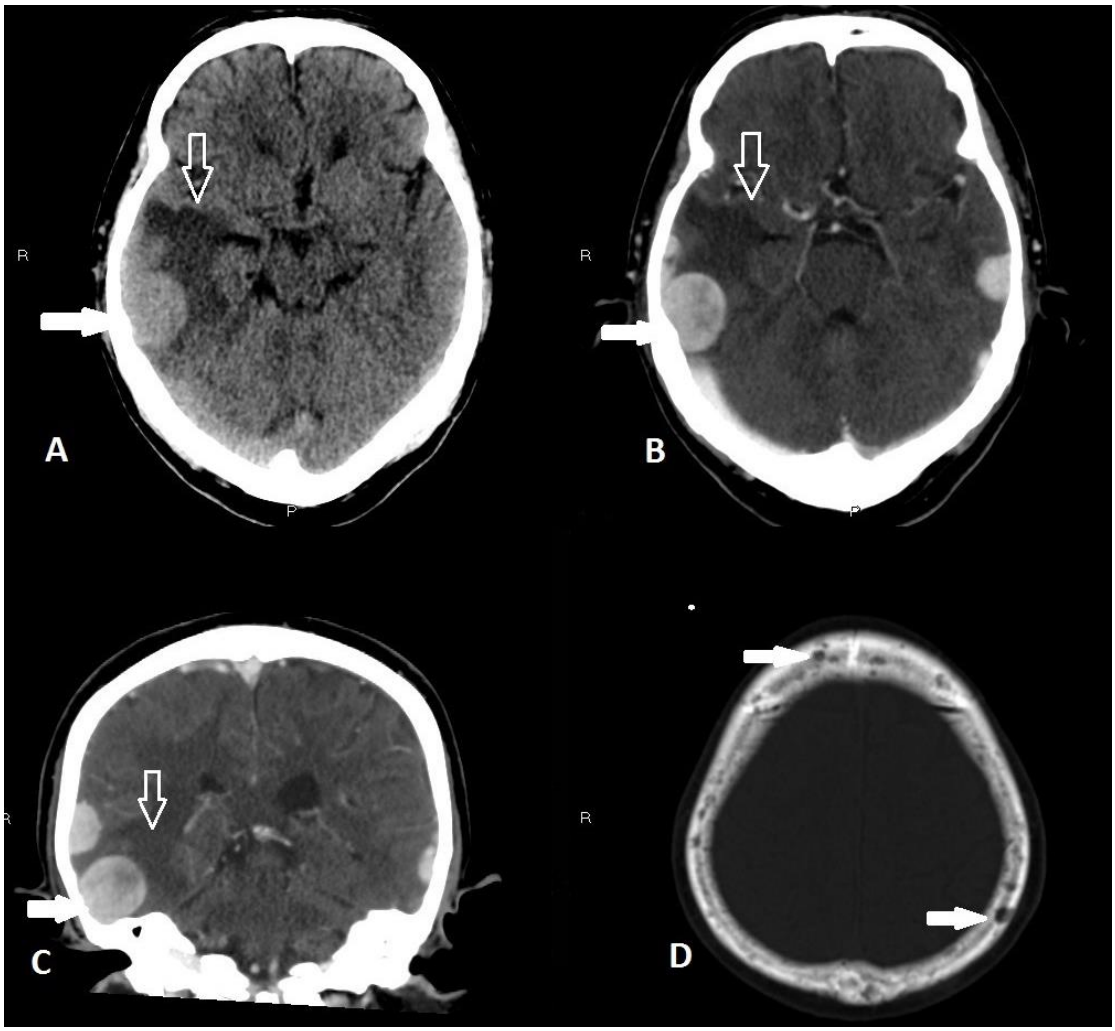

Figure 1: A 64-year-old man with extramedullary multiple myeloma involving multiple organs and the central nervous system. Contrast-enhanced computed tomography of the brain.

FINDINGS: Contrast-enhanced computed tomography (CT) of the brain demonstrates multiple homogeneously enhancing dural based lesions along the cerebral convexities. The largest of the dural based lesions measures 2.5 x 2.7 cm (axial dimensions) along the right middle cranial fossa indenting upon the right temporal lobe (Figure 1A, 1B, 1C, solid arrows). It is associated with surrounding perilesional edema and mass effect (Figure 1A, 1B, 1C, outlined arrows). In addition, there are multiple osteolytic lesions in the calvarium consistent with bony involvement (Figure 1D, solid arrows).

TECHNIQUE: Axial 256 CT scanner, 2160 mAs, 120kV. A total of 50 mLs Omnipaque 350 was administered intravenously. A: Non-contrast axial. B: Contrast-enhanced axial. C: Contrast-enhanced coronal. D: Bone window axial. Slice thickness = 5mm.

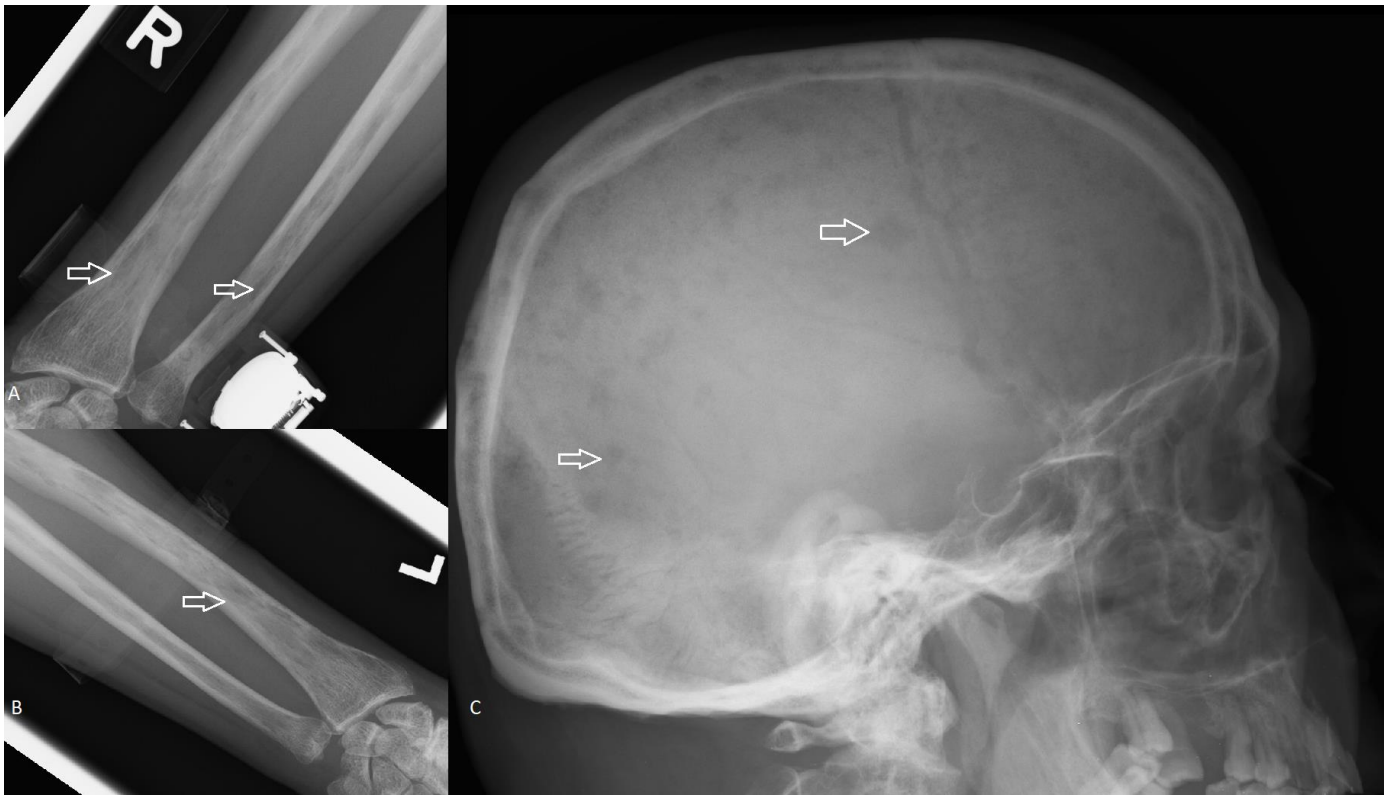

Figure 2: A 64-year-old man with extramedullary multiple myeloma involving multiple organs and the central nervous system. Radiographic skeletal survey.

FINDINGS: Radiographic skeletal survey demonstrates multiple "punched-out" lytic osseous lesions in the bilateral ulnar and radial bones (Figure 2A, 2B, outlined arrows), and skull (Figure 2C, outlined arrow), consistent with bone involvement from multiple myeloma.

TECHNIQUE: A: Antero-posterior radiograph of the right forearm. B: Antero-posterior radiograph of the left forearm. C: Lateral radiograph of the skull.

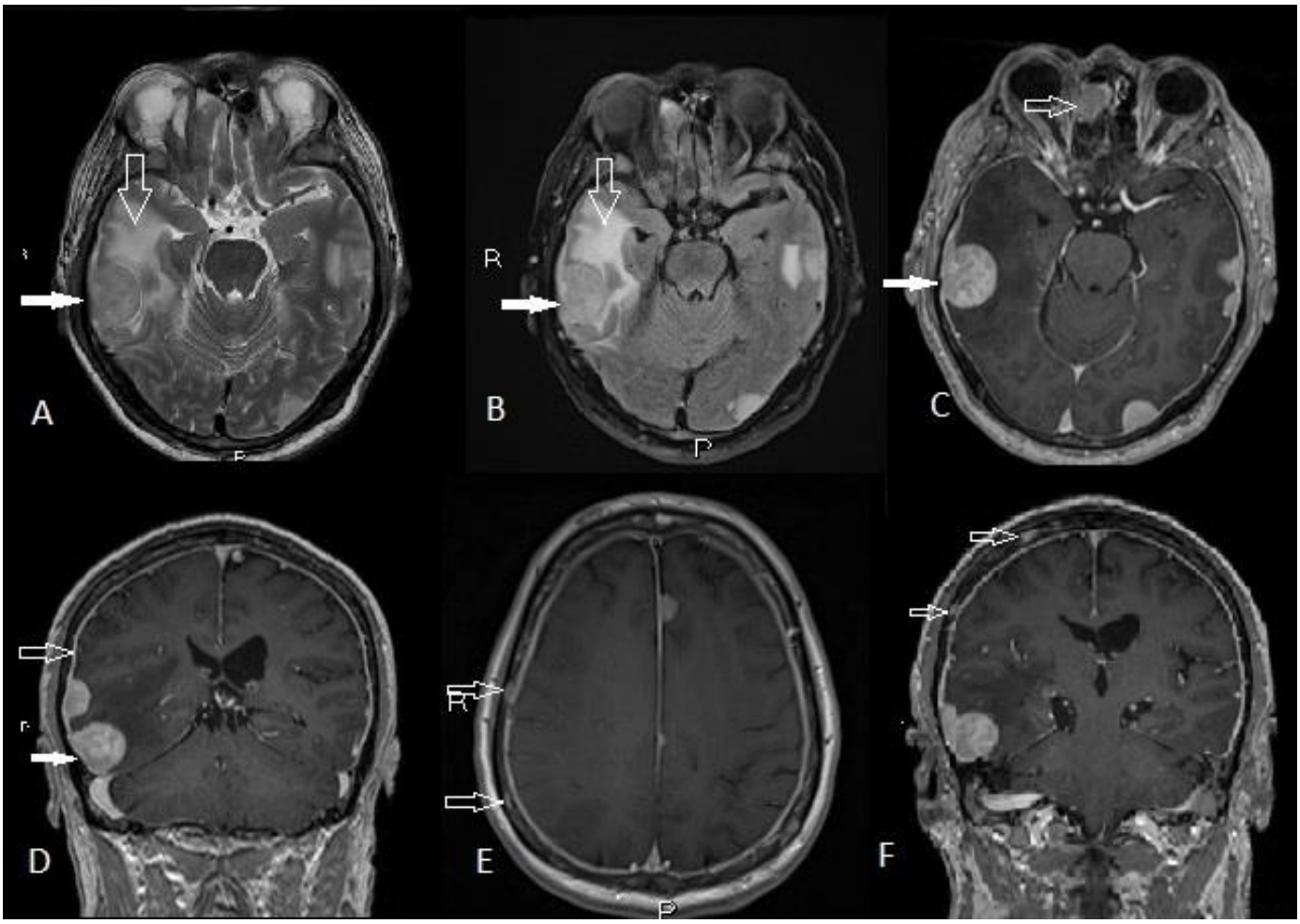

Figure 3: A 64-year-old man with extramedullary multiple myeloma involving multiple organs and the central nervous system. Contrast-enhanced MRI brain.

FINDINGS: MRI brain with axial T2-weighted (Figure 3A), FLAIR (Figure 3B), post-contrast T1-weighted (Figure 3C) images and post-contrast coronal T1-weighted image (Figure 3D) show diffusely thickened linear (Figure 3D, outlined arrow) and nodular enhancement of the pachymeninges (Figure 3D, solid arrow). These nodules are in the supra-tentorial compartment and are entirely extra-axial. The largest of the lesions noted in the right temporal lobe measuring 2.6 x 2.9 cm (axial dimensions) is associated with marked perilesional edema and mass effect (Figure 3A, 3B outlined arrows). In addition, there is a polypoidal centrally enhancing soft tissue mass in the right anterior ethmoid sinus which is consistent with extramedullary soft tissue myeloma (Figure 3C, outlined arrow). Multiple enhancing osseous lesions are scattered throughout the calvarium (Figure 3E, 3F, outlined arrows)

TECHNIQUE: SIEMENS Skyra MRI scanner. Magnetic strength = 3 Tesla. 10 mLs of intravenous Magnevist was administered. A: T2W axial. TR = 4000 ms TE = 92 ms. Slice thickness = 4 mm. B: T2W FLAIR. TR = 6900 ms TE = 132 ms TI= 2192.7 ms. Slice thickness = 4 mm. C, D, F: T1W post-contrast coronal. TR = 1900 ms TE = 2.48 ms TI = 900 ms. Slice thickness = 0.9 mm. E: T1W post-contrast axial. TR = 500 ms TE = 8.4 ms Slice thickness = 4 mm.

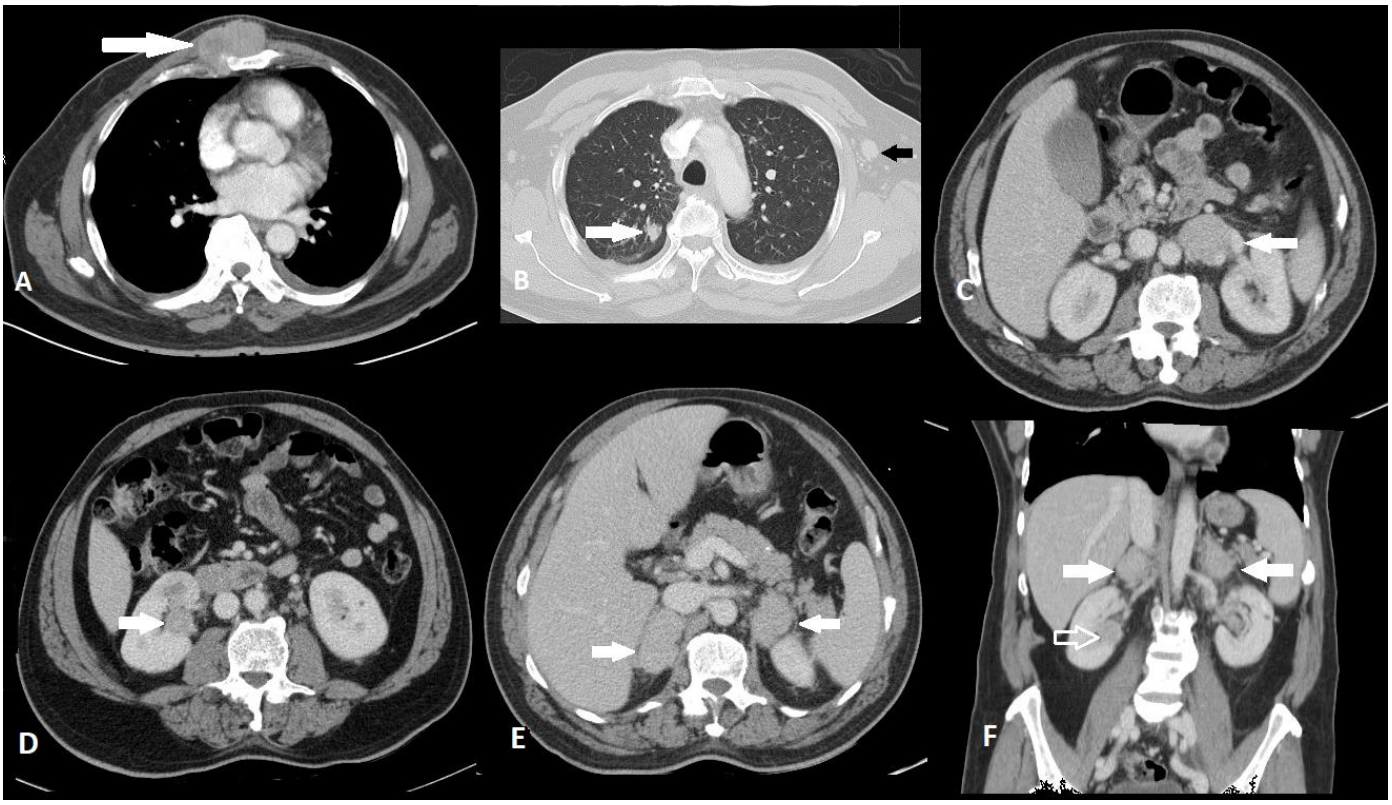

Figure 4: A 64-year-old man with extramedullary multiple myeloma involving multiple organs and the central nervous system. Contrast-enhanced CT of the chest, abdomen and pelvis.

FINDINGS: Contrast-enhanced CT scan of the chest reveals a 4.9 x 2.8 x 3.8 cm (transverse x anterior-posterior x craniocaudal dimensions) soft tissue mass centered within the sternum extending into the soft tissues (Figure 4A, white arrow), several pulmonary nodules, for example, there is a 1.0 x 1.0 x 1.0 cm right upper lobe pulmonary nodule (Figure 4B, white arrow), and left axillary lymphadenopathy measuring 1.2 cm in short-axis dimension (Figure 4B, black arrow). Contrast-enhanced CT abdomen reveals a 2.9 x 3.2 x 3.4 cm soft tissue mass adjacent to the left kidney (Figure 4C, white arrow), a 1.8 x 1.5 x 2.0 cm soft tissue mass inseparable from the right kidney (Figure 4D, white arrow) and lobulated mass lesions in both adrenal glands measuring 2.7 x 4.3 x 3.5 cm on the right and 3.9 x 2.4 x 3.0 on the left (Figure 4E, white arrows). Coronal view of the CT abdomen demonstrates the soft tissue mass in the right kidney (Figure 4E, outlined arrows) and lobulated mass lesions in both adrenal glands (Figure 4E, white arrows). These are consistent with extramedullary multiple myeloma spread.

TECHNIQUE: SIEMENS Sensation axial 256 CT scanner. 6454 mAs, 120kV. A total of 80 mLs Optiray 350 was administered intravenously. A, C, D, E: Contrast-enhanced axial images in soft tissue window. B: Axial lung window. F: Contrast-enhanced coronal image in soft tissue window.

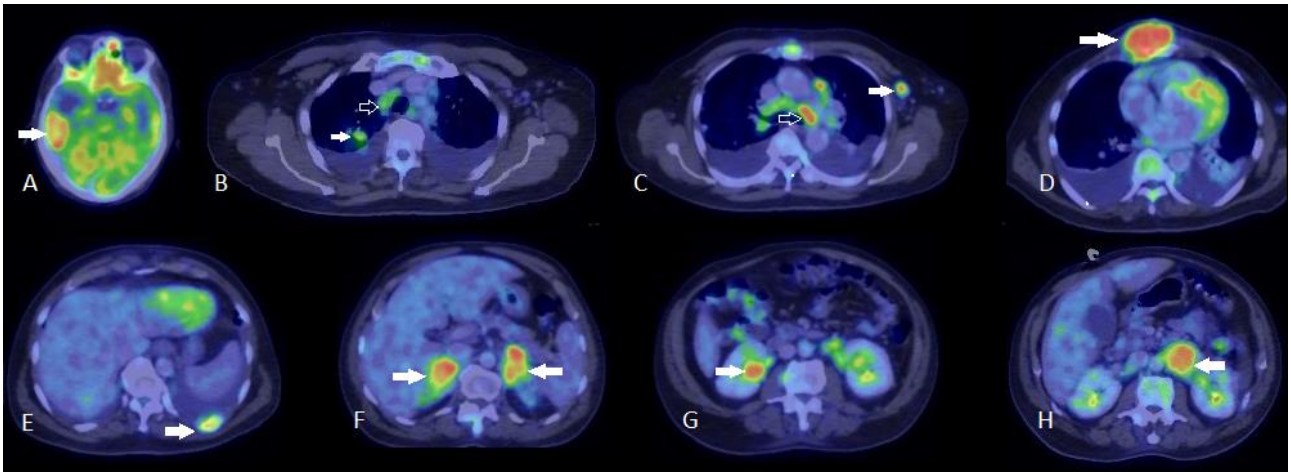

Figure 5: A 64-year-old man with extramedullary multiple myeloma involving multiple organs and the central nervous system. Whole-body positron emission tomography/computed tomography.

FINDINGS: A whole-body positron emission tomography/computed tomography (FDG PET/CT) scan reveals an FDG avid right temporal lobe extra-axial lesion with a SUVmax of 11 (Figure 5A, white arrow). In the thorax, there are FDG avid pulmonary nodules, for example, there is a right upper lobe pulmonary nodule with a SUVmax of 5.1 (Figure 5B, white arrow). FDG avid mediastinal lymph nodes, for example, the right paratracheal lymph node (Figure 5B, outlined arrow) and aortopulmonary lymph node with a SUVmax of 8.3 (Figure 5C, outlined arrow). A left axillary pathological lymph node with a SUVmax of 7.3 (Figure 5C, white arrow). A soft tissue sternal lesion with a SUVmax of 14 (Figure 5D, white arrow). A left tenth rib expansile lesion with a SUVmax of 6.5 (Figure 5E, white arrow). In the abdomen, there are FDG avid bilateral adrenal gland masses (Figure 5F, white arrow) and soft tissues masses adjacent to both kidneys. (Figure 5G, white arrow (right kidney). Figure 5H, white arrow (left kidney)). These findings represent aggressive extramedullary multiple myeloma with multiorgan involvement. Of note, there are bilateral pleural effusions with no uptake, likely reactive.

TECHNIQUE: GE Medical systems Discovery 690. FDG PET/CT imaging was performed from the vertex of the skull to the mid-thigh at 65 minutes after IV administration of 9.5 mCi of F-18 Fluorodeoxyglucose. Contrast-enhanced CT images were acquired simultaneously for anatomical localization and attenuation correction. Slice thickness = 3.75 mm. A-H: Fused FDG PET/CT images were obtained.

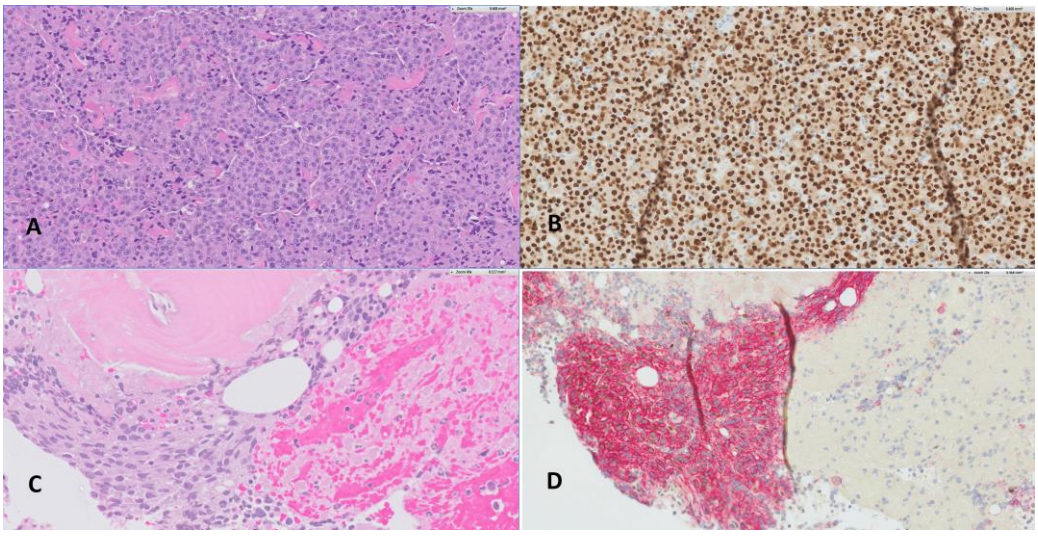

Figure 6: A 64-year-old man with extramedullary multiple myeloma involving multiple organs and the central nervous system. Histology of the sternal mass and bone marrow biopsy.

Findings: Hematoxylin and eosin (H&E) stain (magnification x200) of the sternal mass shows plasmablast-like cells with prominently centrally-nucleolated, eccentric nuclei contained in ample, eosinophilic cytoplasm (Figure 6A). Intense nuclear immunoreactivity for multiple myeloma 1 (MUM1) transcription factor (magnification x200) is also demonstrated (Figure 6B). These findings are compatible with multiple myeloma.
H&E stain at of the bone marrow biopsy (magnification x400) reveals sheets of immature plasma cells occupying approximately 30-40% of the marrow cell population and approximately 20-30% of the inter-trabecular space confirming myeloma (Figure 6C). Strong CD138 expression (magnification x 200) is also demonstrated (Figure 6D). These findings are compatible with multiple myeloma.

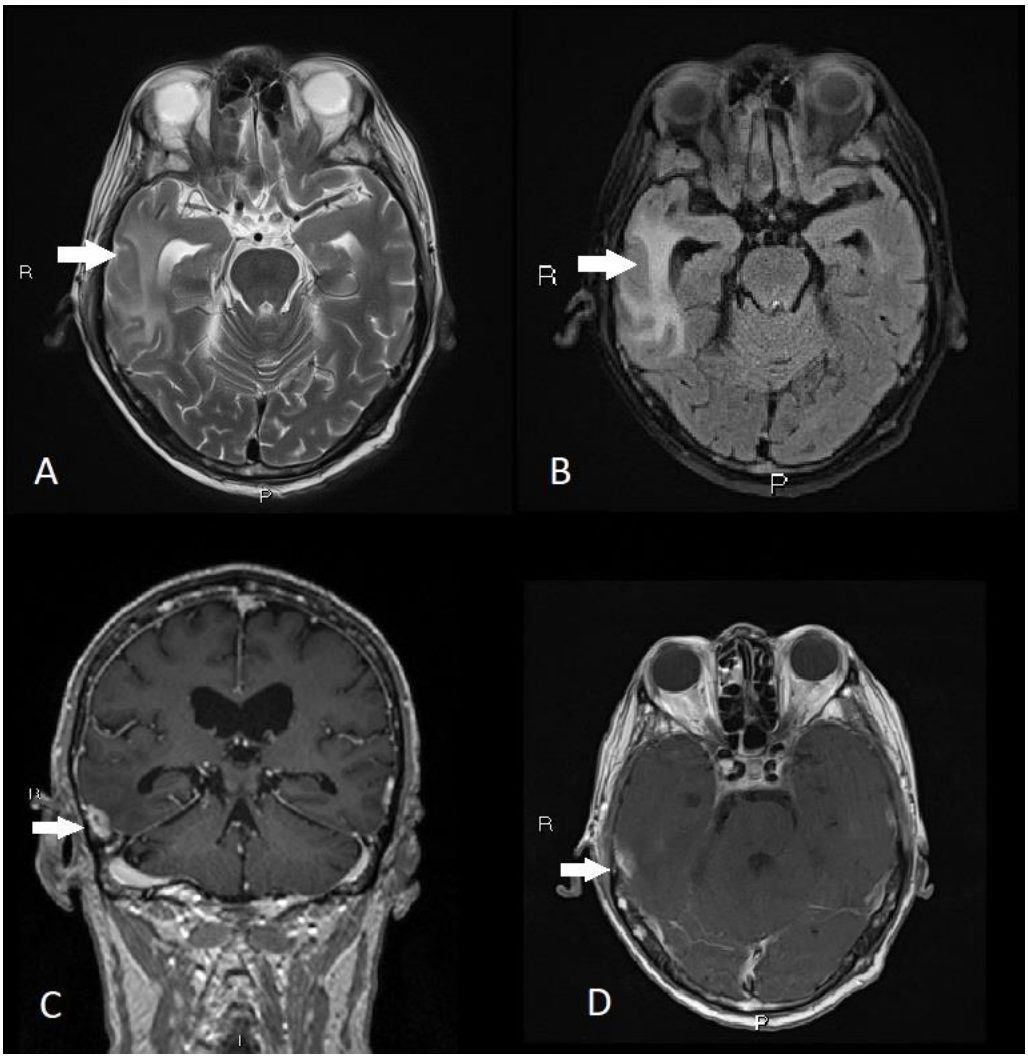

Figure 7: A 64-year-old man with extramedullary multiple myeloma involving multiple organs and the central nervous system. Contrast-enhanced MRI brain approximately 1 month after whole-brain radiotherapy and intrathecal chemotherapy regimen was started.

FINDINGS: MRI brain with axial T2-weighted (Figure 6A), FLAIR (Figure 6B), post-contrast coronal T1-weighted images (Figure 6C) and post-contrast axial T1-weighted image (Figure 6D) show reduction in the nodular enhancement of the pachymeninges after whole-brain radiotherapy and intrathecal chemotherapy regimen. For example, the previously seen largest extra-axial in the right temporal lobe has reduced in size now measuring 1.8 x 0.8 cm (axial dimensions) with decreased perilesional edema and mass effect (white arrows).

TECHNIQUE: SIEMENS Skyra MRI scanner. Magnetic strength = 3 Tesla. 10 mLs of intravenous Magnevist was administered. A: T2W axial. TR = 5520 ms TE = 100 ms. Slice thickness = 4 mm. B: T2W FLAIR. TR = 6610 ms TE = 106 ms TI= 2139.2 ms. Slice thickness = 4 mm. C: T1W post-contrast coronal. TR = 1700 ms TE=2.43 ms TI = 900 ms. Slice thickness = 1 mm. D: T1W post-contrast axial. TR = 526 ms T = 9.3 ms. Slice thickness = 4 mm.

Etiology	• Multiple myeloma (MM) is a hematologic malignancy secondary to monoclonal proliferation of bone marrow plasma cells. • MM is usually confined to the bone marrow, although extramedullary involvement is known to occur in almost any organ system. • Myelomatous spread to the central nervous system is a rare manifestation of MM.
Incidence	• MM has an incidence of 2.1 per 100 000 persons. • Extramedullary MM can involve any systemic organ and is seen in 10-16% of multiple myeloma cases. • Central nervous system (CNS) involvement is only seen in 0.7% of multiple myeloma cases.
Gender	• Intramedullary multiple myeloma has a slight male predilection. • Extramedullary multiple myeloma (EM) has a higher male to female ratio than intramedullary MM (1.9 vs 1.1, respectively).
Age predilection and risk factors	• Median age of presentation for MM is 66 years. • Risk factors include: advanced age, African American ethnicity, family history of MM, obesity, history of MGUS or solitary plasmacytoma.
Imaging findings	• MM show multiple "punched-out' lytic osseous lesions scattered throughout the axial and appendicular skeletons on CT and MRI. • The lesions demonstrate hypermetabolism on FDG PET/CT. • The imaging appearance of EM is typically that of homogeneous soft tissues masses on cross-sectional imaging, involving the reticuloendothelial system, abdominal organs such as the kidneys and small bowel, and head and neck region. Less commonly, it affects the chest as parenchymal nodules or masses, interstitial infiltration and pleural deposits. • Intracranial manifestations of CNS multiple myeloma on CT and MRI are pachymeningeal and leptomeningeal enhancing deposits, intraparenchymal brain lesions and direct extra-axial extension.
Treatment	• Combination of conventional chemotherapy, proteasome inhibitors, immunomodulatory imide drugs, autologous stem cell transplant and radiotherapy are often used. • In the case of EM with CNS involvement, the use of craniocaudal irradiation and intrathecal and systemic combinational chemotherapy that crosses the blood-brain barrier hence allowing CNS penetration is advocated.
Prognosis	• EM has a poor prognosis with an overall survival rate of 6 months during relapse, • Median survival of MM patients with CNS involvement is 3.4 months.

Table 1: Summary table of extramedullary multiple myeloma with central nervous involvement

	MRI	CT
Central nervous system multiple myeloma	• T1W isointense. • T2W hyperintense. • No restricted diffusion. Diffusely thickened linear or nodular enhancing pachymeninges.	• Diffusely thickened linear or nodular enhancing pachymeninges.
Dural metastases	• T1W hypointense. T2W hyperintense. No restricted diffusion. • Linear or nodular enhancement of the pachymeninges.	• Linear or nodular enhancement of the pachymeninges.
Primary dural lymphoma	• T1W isointense. T2W hypointense. Restricted diffusion. • Single or multiple diffusely enhancing dural based extraaxial masses.	• Single or multiple diffusely enhancing dural based extraaxial masses.
Primary dural based intracranial tumors with extra-neural spread such as solitary fibrous tumors	• T1W hypointense. • T2W hyperintense. • No restricted diffusion. • Large extraaxial multilobulated mass lesion with homogeneous or heterogeneous enhancement.	• Large extraaxial multilobulated mass lesion with homogeneous or heterogeneous enhancement. In contrast to meningiomas, they usually lack hyperostosis and calcification.
Neurosarcoidosis	• T1W iso- to hypo-intense. • T2W hypointense. • No restricted diffusion. • Leptomeningeal enhancement is more common than pachymeningeal disease.	• Diffuse and nodular enhancing leptomeninges or pachymeninges.
Hypertrophic pachymeningitis	• T1W hypointense. T2W hypointense. • No restricted diffusion. • Pachymeningeal nodular enhancement.	• Hyperdense diffuse and nodular pachymeninges with corresponding homogeneous enhancement.

Table 2: Differential diagnosis table for pachymeningeal disease

ABBREVIATIONS

CNS = central nervous system
CT = computed tomography
EM = extramedullary multiple myeloma
FDG PET/CT = 18F-Fluorodeoxyglucose positron emission tomography/computed tomography
FDG = 18F-Fluorodeoxyglucose
MGUS = monoclonal gammopathy of undetermined significance
MM = multiple myeloma
MRI = magnetic resonance imaging

KEYWORDS

Central nervous system multiple myeloma; extraosseous multiple myeloma; extramedullary multiple myeloma; multiple myeloma; pachymeningeal disease

ACKNOWLEDGEMENTS

Dr Amos Tay Zhi En from the Department of Pathology, Singapore General Hospital. For providing the histology slides.